(2002)

OL-CR 1

8.1.10

Collapse and revival of the matter wave field of a Bose–Einstein condensate

Markus Greiner, Olaf Mandel, Theodor W. Hänsch & Immanuel Bloch

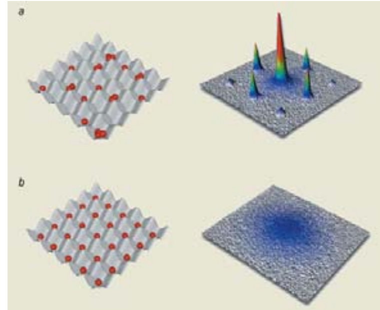

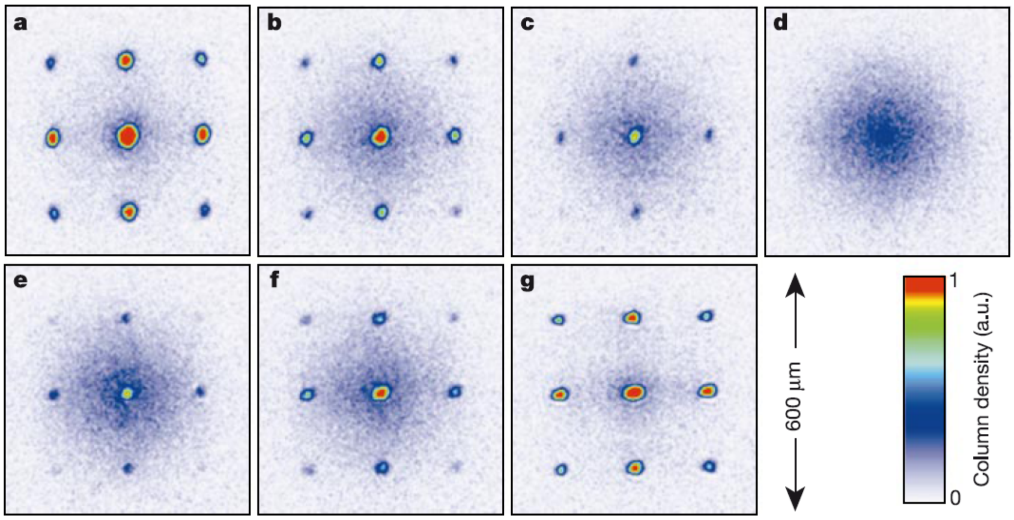

OL-CR 2

Figure 2 Dynamical evolution of the multiple matter wave interference pattern observed after jumping from a potential depth $V_A = 8\ E_r$ to a potential depth $V_B = 22\ E_r$ and a subsequent variable hold time t. After this hold time, all trapping potentials were shut off and absorption images were taken after a time-of-flight period of 16 ms. The hold times t were **a**, 0 μs; **b**, 100 μs; **c**, 150 μs; **d**, 250 μs; **e**, 350 μs; **f**, 400 μs; and **g**, 550 μs. At first, a distinct interference pattern is visible, showing that initially the system can be described by a macroscopic matter wave with phase coherence between individual potential wells. Then after a time of ~250 μs the interference pattern is completely lost. The vanishing of the interference pattern is caused by a collapse of the macroscopic matter wave field in each lattice potential well. But after a total hold time of 550 μs (**g**) the interference pattern is almost perfectly restored, showing that the macroscopic matter wave field has revived. The atom number statistics in each well, however, remains constant throughout the dynamical evolution time. This is fundamentally different from the vanishing of the interference pattern with no further dynamical evolution, which is observed in the quantum phase transition to a Mott insulator, where Fock states are formed in each potential well. From the above images the number of coherent atoms N_{coh} is determined by first fitting a broad two-dimensional gaussian function to the incoherent background of atoms. The fitting region for the incoherent atoms excludes 130 μm × 130 μm squares around the interference peaks. Then the number of atoms in these squares is counted by a pixel-sum, from which the number of atoms in the incoherent gaussian background in these fields is subtracted to yield N_{coh}. a.u., arbitrary units.

OL-CR 3

$$H = -J\sum_{\langle i,j\rangle}\hat{a}_i^\dagger \hat{a}_j + \sum_i \epsilon_i \hat{n}_i + \frac{1}{2}U\sum_i \hat{n}_i(\hat{n}_i - 1)$$

$$H_{eff} = -J\sum_{\langle ij\rangle} a_j^\dagger a_j \qquad\qquad H_{eff} = \frac{1}{2}U\sum_i \hat{n}_i(\hat{n}_i - 1)$$

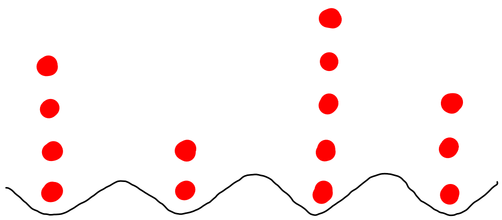

$J \gg U$

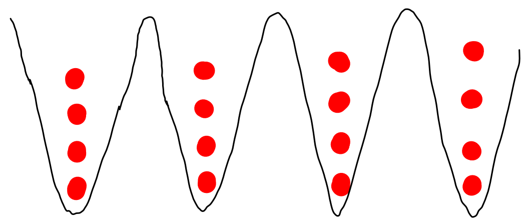

$J \ll U$

$J \gg U$: $\quad |\Psi_{SF}\rangle_{U=0} \propto \left(\sum_{i=1}^{M} \hat{a}_i^\dagger\right)^N |0\rangle$

Superfluid

$J \ll U$: $\quad |\Psi_{MI}\rangle_{J=0} \propto \prod_{i=1}^{M} (\hat{a}_i^\dagger)^n |0\rangle$, $\quad M$ = lattice sites

Mott-Insulator

for $N = L \cdot M$

OL-CR 4

Dynamics of single site if $U \gg J$

$$H_{eff} = \frac{1}{2}U\, n(n-1) =: E_n$$

Consider Number eigenstate: $\quad \hat{N}|n\rangle = n|n\rangle$

$$|n(t)\rangle = e^{-iH_{eff}t/\hbar}|n\rangle(0) = e^{-i/2\, U n(n-1)\, t/\hbar}\,|n\rangle(0)$$

Consider Coherent state: $\quad a|\alpha\rangle = \alpha|\alpha\rangle$

$$|\alpha(0)\rangle = e^{-|\alpha|^2/2}\sum_{n=1}^{\infty}\frac{\alpha^n}{\sqrt{n!}}|n\rangle$$

$$|\alpha(t)\rangle = e^{-iH_{eff}t/\hbar}|\alpha\rangle = e^{-|\alpha|^2/2}\sum_{n=1}^{\infty}\frac{\alpha^n}{\sqrt{n!}}\, e^{-i\frac{1}{2}U n(n-1)t\frac{2\pi}{h}}|n\rangle$$

$$= |\alpha(0)\rangle \quad \text{for} \quad t = m h/U, \quad \text{since } e^{-i n(n-1)\pi} = 1$$

OL-CR5

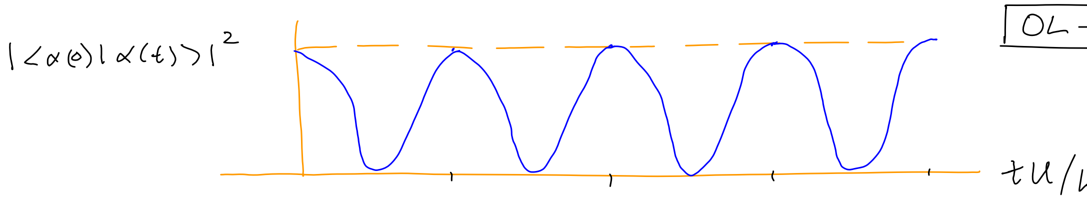

For an arbitrary other coherent state $|\beta\rangle$:

$$|\langle\beta|\alpha(t)\rangle|^2 = e^{-(|\beta|^2+|\alpha|^2)/2} \sum_{n=1}^{\infty} \frac{(\beta^*\alpha)^n}{n!} \underbrace{e^{-in(n-1)\pi\, Ut/h}}_{=1 \text{ for } t = m\, h/U}$$

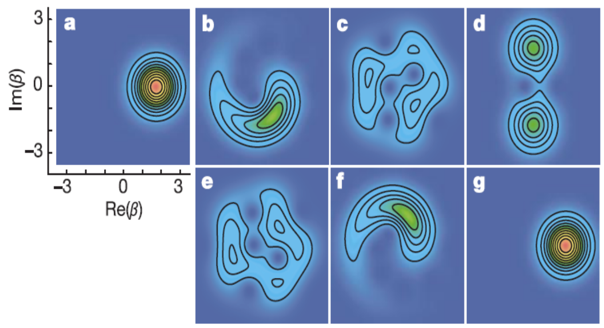

Figure 1 Quantum dynamics of a coherent state owing to cold collisions. The images **a**–**g** show the overlap $|\langle\beta|\alpha(t)\rangle|^2$ of an arbitrary coherent state $|\beta\rangle$ with complex amplitude β with the dynamically evolved quantum state $|\alpha\rangle(t)$ (see equation (2)) for an average number of $|\alpha|^2 = 3$ atoms at different times t. **a**, $t = 0\,h/U$; **b**, 0.1 h/U; **c**, 0.4 h/U; **d**, 0.5 h/U; **e**, 0.6 h/U; **f**, 0.9 h/U; and **g**, h/U. Initially, the phase of the macroscopic matter wave field becomes more and more uncertain as time evolves (**b**), but remarkably at $t_{rev}/2$ (**d**), when the macroscopic field has collapsed such that $\psi \approx 0$, the system has evolved into an exact 'Schrödinger cat' state of two coherent states. These two states are 180° out of phase, and therefore lead to a vanishing macroscopic field ψ at these times. More generally, we can show that at certain rational fractions of the revival time t_{rev}, the system evolves into other exact superpositions of coherent states—for example, at $t_{rev}/4$, four coherent states, or at $t_{rev}/3$, three coherent states[2,4]. A full revival of the initial coherent state is then reached at $t = h/U$. In the graph, red denotes maximum overlap and blue vanishing overlap with 10 contour lines in between.

OL-CR6

More generally, for any local superposition:

$$|\psi(0)\rangle = \sum_n A_n |n\rangle$$

$$|\psi(t)\rangle = \sum_n A_n\, e^{-i\, n(n-1)\pi\, Ut/h} |n\rangle$$

$$|\langle\psi(0)|\psi(t)\rangle|^2 = \sum_n |A_n|^2\, e^{-i\, n(n-1)\pi\, Ut/h}$$

$$= 1 \quad \text{for} \quad t = m\, t_{rev}, \quad \text{with} \quad t_{rev} = h/U = \text{revival time}$$

$\Rightarrow$ local wave function that is superposition of <u>number</u> <u>states</u> and evolves under $H = \frac{U}{2} n(n-1)$, shows "collapse" after $\frac{t_{rev}}{2}$ and "revival" after $t_{rev} = h/U$

OL - CR 7

Experimental protocol:

$$H_{eff} = \sum_i \tfrac{1}{2} U n_i (n_i - 1)$$

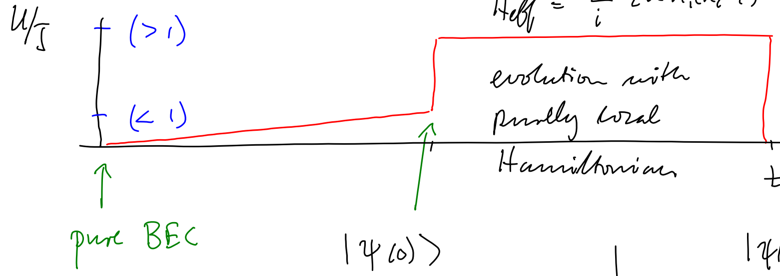

open trap, start time of flight measurement

$|\psi(0)\rangle$

$$\simeq \left(\sum_{i=1}^{M} a_i^\dagger \right)^N |0\rangle$$

$$\simeq \prod_{i=1}^{M} \underbrace{|\psi(0)\rangle_i}_{\sum_{n=0}^{\infty} A_n |n\rangle_i}$$

all sites are described by same wavefunction, "almost a coherent state"

$|\psi(t)\rangle$

$$= \prod_{i=1}^{M} \underbrace{|\psi(t)\rangle_i}_{\sum_{n=0}^{\infty} e^{-i n(n-1)\pi \frac{Ut}{h}} |n\rangle_i}$$

$$\simeq |\psi(0)\rangle \quad \text{for } t = m\, t_{rev}$$

$\Rightarrow$ revivals are seen, see p. 11

OL - CR 8

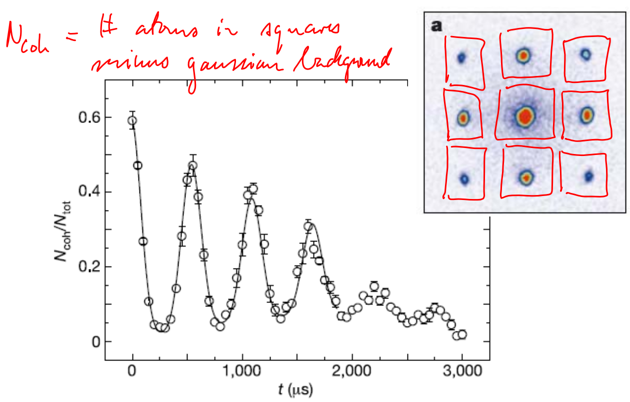

Figure 3 Number of coherent atoms relative to the total number of atoms monitored over time for the same experimental sequence as in Fig. 2. The solid line is a fit to the data assuming a sum of gaussians with constant widths and constant time separations, including an exponential damping and a linear background. The damping is mainly due to the following process: after jumping to a potential depth V_B and thereby abruptly changing the external confinement and the on-site matrix element U, we obtain a parabolic profile of the chemical potential over the cloud of atoms in the optical lattice, which leads to a broadening of the interference peaks over time. When the interference peaks become broader than the rectangular area in which they are counted, we cannot determine N_{coh} correctly any more, which explains the rather abrupt damping that can be seen—for example, between the third and fourth revival in the above figure. Furthermore, the difference in U of ~3% over the cloud of atoms contributes to the damping of N_{coh}/N_{tot} over time. The finite contrast in N_{coh}/N_{tot} of initially 60% can be attributed to atoms in higher-order momentum peaks (~10% of the total atom number), s-wave scattering spheres created during the expansion[14], a quantum depletion of the condensate for the initial potential depth of $V_A = 8\ E_r$, and a finite condensate fraction due to the finite temperature of the system.

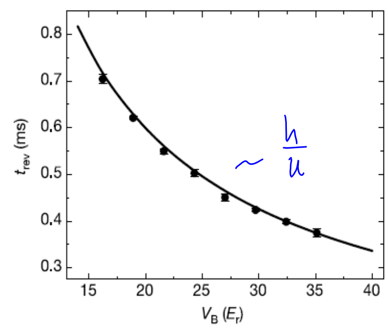

Figure 4 Revival period in the dynamical evolution of the interference pattern after jumping to different potential depths V_B from a potential depth of $V_A = 5.5\ E_r$. The solid line is an *ab initio* calculation of h/U with no adjustable parameters based on a band structure calculation. In addition to the statistical uncertainties shown in the revival times, the experimental data points have a systematic uncertainty of 15% in the values for the potential depth.